

Rational Design of Three-Dimensional (3D) Optically Active Molecule-Based Magnets: Synthesis, Structure, Optical and Magnetic Properties of $\{[\text{Ru}(\text{bpy})_3]^{2+}, \text{ClO}_4^-, [\text{Mn}^{\text{II}}\text{Cr}^{\text{III}}(\text{ox})_3]^{-}\}_n$ and $\{[\text{Ru}(\text{bpy})_2\text{ppy}]^+, [\text{M}^{\text{II}}\text{Cr}^{\text{III}}(\text{ox})_3]^{-}\}_n$, with $\text{M}^{\text{II}} = \text{Mn}^{\text{II}}, \text{Ni}^{\text{II}}$. X-ray Structure of $\{[\Delta\text{Ru}(\text{bpy})_3]^{2+}, \text{ClO}_4^-, [\Delta\text{Mn}^{\text{II}}\Delta\text{Cr}^{\text{III}}(\text{ox})_3]^{-}\}_n$ and $\{[\Lambda\text{Ru}(\text{bpy})_2\text{ppy}]^+, [\Lambda\text{Mn}^{\text{II}}\Lambda\text{Cr}^{\text{III}}(\text{ox})_3]^{-}\}_n$

Román Andrés,[†] Muriel Brissard,[†] Michel Gruselle,^{*,†} Cyrille Train,[†] Jacqueline Vaissermann,[†] Bernard Malézieux,[†] Jean-Pierre Jamet,[‡] and Michel Verdaguer[†]

Laboratoire de Chimie Inorganique et Matériaux Moléculaires, CIM² Unité CNRS 7071, Université Pierre et Marie Curie, 4 place Jussieu, case 42, 75252 Paris Cedex 05, France, and Laboratoire de Physique des Solides, UMR 850, Université Paris Sud (Paris XI), bât. 510, 91405 Orsay Cedex, France

Received April 3, 2001

To elucidate the relation between structural and magnetic properties, we have synthesized molecular materials having both Cotton effects and a ferromagnetic long range order. Such optically active 3D molecule-based magnets were rationally designed using the enantioselective template effect of optically active cations, namely Δ or Λ $[\text{Ru}(\text{bpy})_3, \text{ClO}_4]^+$ or Δ or Λ $[\text{Ru}(\text{bpy})_2\text{ppy}]^+$ (bpy = bipyridine; ppy = phenylpyridine). Such cations are able to template the formation of optically active 3D anionic networks in which transition metal ions (Cr–Mn) and (Cr–Ni) are connected by oxalate ligands (ox). Following this strategy, we described the synthesis of $\{[\text{Ru}(\text{bpy})_3]^{2+}, \text{ClO}_4^-, [\text{Mn}^{\text{II}}\text{Cr}^{\text{III}}(\text{ox})_3]^{-}\}_n$ and $\{[\text{Ru}(\text{bpy})_2\text{ppy}]^+, [\text{M}^{\text{II}}\text{Cr}^{\text{III}}(\text{ox})_3]^{-}\}_n$ with $\text{M}^{\text{II}} = \text{Mn}^{\text{II}}, \text{Ni}^{\text{II}}$ in their optically active forms. In these 3D networks, all of the metallic centers have the same configuration, Δ or Λ , as the template cation. We have determined the structure of $\{[\Delta\text{Ru}(\text{bpy})_3][\text{ClO}_4][\Delta\text{Mn}\Delta\text{Cr}(\text{ox})_3]\}_n$ and $\{[\Lambda\text{Ru}(\text{bpy})_2\text{ppy}]^+, [\Lambda\text{Mn}^{\text{II}}\Lambda\text{Cr}^{\text{III}}(\text{ox})_3]^{-}\}_n$ by X-ray diffraction studies. These optically active networks show the Cotton effect and long-range ferromagnetic order at low temperatures. The magnetic circular dichroism of $\{[\text{Ru}(\text{bpy})_3]^{2+}, \text{ClO}_4^-, [\text{Mn}^{\text{II}}\text{Cr}^{\text{III}}(\text{ox})_3]^{-}\}_n$ at 2 K is reported.

Introduction

The need for new materials that have more diversified and more sophisticated properties is continuously increasing.¹ Opportunities offered by the flexibility of inorganic molecular chemistry has recently led to a blossoming of new research fields in inorganic molecular materials. One of the goals is to obtain materials that possess not only one expected property (mechanical, optical, magnetic, electric...) or function (rigidity, transparency, conductivity...) but also combine two or more of them in polyfunctional systems, for instance, superconducting paramagnets,² photomagnetic ferrimagnets,³ and transparent room-temperature magnets.⁴ Along these lines, we describe the synthesis and the characterization of the first 3D optically active molecule-based magnets. It is noteworthy that chiral magnets obtained in a racemic way were recently described by Gatteschi,⁵ Inoue,⁶ Julve,⁷ and Coronado.⁸ We first review the previous endeavors in the field of chiral magnets. We then propose a

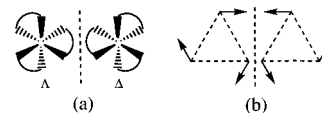


Figure 1. Illustrative examples of (a) structural and (b) magnetic chiralities.

general strategy used to overcome structural, kinetic, and entropic hindrances and to obtain the desired structures and magnetism. The presentation of structural, optical, magnetic, and magneto-optical results is followed by a brief discussion of the prospects opened by our findings for understanding the relationship between chirality and spin organization and for observing new physical effects.

Chirality is a well-known concept for chemists.⁹ For them, it is associated with a loss of mirror symmetry at the molecular level (see Figure 1a). This loss of symmetry gives rise to natural circular dichroism (NCD) in solutions or solids containing such asymmetric units.

Physicists have recently introduced the concept of chirality in magnetic materials.¹⁰ It appears in CsMX_3 (with $\text{M} = \text{Mn}$,

* To whom correspondence should be addressed.

[†] Université Pierre et Marie Curie.

[‡] Université Paris Sud (Paris XI).

(1) Kahn, O. *Molecular Magnetism*; VCH: Weinheim, 1993.

(2) Kurmoo M.; Graham, A. W.; Day, P.; Coles, S. J.; Hursthouse, M. B.; Caulfield, J. L.; Singleton, J.; Pratt, F. L.; Hayes, W.; Ducasse, L.; Guionneau, P. *J. Am. Chem. Soc.* **1995**, *117*, 12209–12217.

(3) Sato, O.; Iyota, T.; Fujishima, A.; Hashimoto, K. *Science* **1996**, *272*, 704–705.

(4) Ferlay, S.; Mallah, T.; Ouahes, R.; Veillet, P.; Verdaguer, M. *Nature* **1995**, *378*, 701–703.

(5) Caneschi, A.; Gatteschi, D.; Ray, P.; Sessoli, R. *Inorg. Chem.* **1991**, *30*, 3936–3941.

(6) Kumaiga, H.; Inoue, K. *Angew. Chem., Int. Ed. Engl.* **1999**, *38*, 1601–1603.

(7) Hernandez-Molina, M.; Lloret, F.; Ruiz-Pérez, C.; Julve, M. *Inorg. Chem.* **1998**, *37*, 4131–4135.

(8) Coronado, E.; Galan-Mascaros, J. R.; Gomez-Garcia, C. J.; Martinez-Agudo, J. M. *Inorg. Chem.* **2001**, *40*, 113–120.

(9) Jacques, J.; Collet, A.; Wilen, S. H. *Enantiomers, Racemates and Resolution*; John Wiley & Sons: New York, 1981.

(10) Kawamura H. *J. Phys. Soc. Jpn.* **1985**, *54*, 3220.

Ni, Cu; and X = Cl, Br) compounds which are quasi-1D ferromagnets which order antiferromagnetically at low temperature because of interchain interaction. Magnetic chirality comes from frustration effects arising from the antiferromagnetic interaction in the triangular spin system of these compounds (see Figure 1 b).¹¹ Moreover, in CsCuCl₃, a helical spin organization inside the chain is superimposed to the triangular magnetic structure within the plane. Adachi et al.¹¹ related the magnetic helicity to the structural helicity arising from cooperative Jahn–Teller effect at low temperature. Their hypothesis concerning the link between the two helicities remains an open question since these chiral crystals are obtained through spontaneous resolution processes, e.g., without precise control over structural chirality.

Our work deals with ferromagnetic compounds in which the mirror symmetry is lost both at the molecular level and in the crystal structure. To avoid the confusion between the two definitions of chirality given above, the former will be referred to as “structural chirality” while the latter will be called “magnetic chirality”.¹²

The synthesis of well-defined solid structures possessing both ferro- or ferrimagnetic order and optical activity represents a challenge in materials science. Coordination chemistry offers great possibilities for the design of such polymeric compounds.¹³ In particular, the oxalate ligand (C₂O₄)²⁻ is well known for bridging two metal centers with significant exchange interactions, whereby each metal remains hexacoordinated and possesses a propeller-like chiral structure of D₃ symmetry with a predetermined twist.

In the past few years Okawa, Decurtins, Day, Coronado, Atovmyan, and Clement have thoroughly investigated two- and three-dimensional networks (noted as 2D and 3D) prepared from the combination of tris(oxalato)metalates, such as [Cr^{III}(ox)₃]³⁻,¹⁴ with other metallic species, such as alkali monocations (Li⁺, Na⁺) or dicationic transition metal ions (Mn²⁺, Ni²⁺, Fe²⁺).^{15–20} These bimetallic networks have the general formula [A^{x+}, [M₁M₂(ox)₃]^{x-}]_n; they can be described as being composed of an anionic sublattice [[M₁M₂(ox)₃]^{x-}]_n and a cationic counterpart (A^{x+})_n. The charge of each repeating unit of the anionic sublattice is one or two depending on the oxidation states of

the metal centers. Since the previous research investigations²¹ were carried out on racemic mixtures, one would expect to obtain only racemic materials. However, in some rare cases, spontaneous resolution may occur during the crystallization process, leading to a mixture of enantiomerically pure or twinned crystals.²² Nevertheless, this method cannot be considered as a systematic way to prepare pure resolved materials.⁹

In the present work, we explore the enantioselective synthesis of optically active three-dimensional oxalate-bridged networks using resolved [Cr(ox)₃]³⁻ as anionic bricks or [Ru(bpy)₃]²⁺ and/or [Ru(bpy)₃ppy]⁺ as template cations. We report herein the results of the synthesis and characterization and the optical and magnetic behaviors of compounds {[Ru(bpy)₃]²⁺, ClO₄⁻, [Mn^{II}Cr^{III}(ox)₃]⁻]_n **1** and {[Ru(bpy)₂ppy]⁺, [M^{II}Cr^{III}(ox)₃]⁻]_n, M^{II} = Mn^{II} **2**, Ni^{II} **3**, with bpy = bipyridine, ppy = phenylpyridine, and ox = C₂O₄²⁻. X-ray diffraction studies were performed for {[ΔRu(bpy)₃]²⁺, ClO₄⁻, [ΔMn^{II}ΔCr^{III}(ox)₃]⁻]_n **1-Δ** and {[ΛRu(bpy)₂ppy]⁺, [ΛMn^{II}ΛCr^{III}(ox)₃]⁻]_n **2-Λ**.

Experimental Section

Materials. The following complexes were prepared according to the literature methods: A₃Cr(ox)₃·3H₂O (A = K, NH₄),²³ [Ru(bpy)₃]-X₂ (X = Cl, I, ClO₄),²⁴ and [Ru(bpy)₂ppy]PF₆.²⁵ Procedures of resolution, already described, have been followed to obtain enantiomerically pure or enriched Δ and Λ isomers of [Cr(ox)₃]³⁻,²⁶ [Ru(bpy)₃]²⁺,²⁷ and [Ru(bpy)₂ppy]⁺.²⁸ The other reagents are commercially available and were used as purchased.

Physical Techniques. The IR spectra were recorded on a Bio-Rad IRFT spectrophotometer as KBr pellets in the 4000–250 cm⁻¹ region. Elemental analyses were completed at the SIAR–UPMC, Paris. Metal analyses were performed at the Service Central d'Analyse-CNRS, Vernaison. Specific rotations of the starting materials were measured at 20 °C, in a 1 dm tube containing the aqueous solution, using the sodium D line in a polarimeter America A A5. The enantiomeric excesses were calculated by comparison with the maximum specific rotation values found in the literature. Circular dichroism spectra were measured with a Jasco model J-710 spectropolarimeter. Measurements were made on the resulting complexes as dispersions of 0.1–1 mg in 100 mg of oven-dried KBr. Thirteen millimeter diameter disks were made in a standard disk press. The baseline correction was performed with the spectrum of a pure KBr disk. The displayed absorption spectra result from subtraction of spectrum of a standard KBr disk.

The magnetic moment of powdered samples were measured between 2 and 300 K on a Quantum Design MPMS5 squid magnetometer. The hysteresis loops are measured at 2 K. The zero field cooled (ZFC), field cooled (FC), and remnant magnetization versus temperature are measured in a 0.01 T external field. The susceptibility is measured in a 0.1 T external field and corrected for diamagnetism and temperature independent paramagnetism.

The magnetic circular dichroism (MCD) was measured on a homemade apparatus using photoelastic modulation. The light source

- (11) Adachi, K.; Achiwa N.; Mekata, M. *J. Phys. Soc. Jpn.* **1980**, *49*, 545–553.
 (12) Barron, L. D. *Nature* **2000**, *405*, 895–896.
 (13) (a) Von Zelewsky, A.; Mamula, O. *J. Chem. Soc., Dalton Trans.* **2000**, 219–231. (b) Keene, F. R. *Coord. Chem. Rev.* **1997**, *166*, 121–159. (c) Tzalis, D.; Tor, Y. *J. Am. Chem. Soc.* **1997**, *119*, 852–853.
 (14) The tris(oxalato)chromate (III) ion, [Cr(ox)₃]³⁻, was the first resolved anion. Werner, A. *Ber.* **1912**, *45*, 3061–3070.
 (15) (a) Zhong, Z. J.; Matsumoto, N.; Okawa, H.; Kida, S. *Chem. Lett.* **1990**, 87–90. (b) Tamaki, H.; Zhong, Z. J.; Matsumoto, N.; Kida, S.; Koikawa, M.; Achiwa, N.; Hashimoto, Y.; Okawa, H. *J. Am. Chem. Soc.* **1992**, *114*, 6974–6979.
 (16) (a) Decurtins, S.; Schmalte, H. W.; Oswald, H. R.; Linden, A.; Ensling, J.; Gütlich, P.; Hauser, A. *Inorg. Chim. Acta* **1994**, *216*, 65–73. (b) Pellaux R.; Schmalte, H. W.; Huber, R.; Fischer, P.; Hauss, T.; Ouladdiaf, B.; Decurtins, S. *Inorg. Chem.* **1997**, *36*, 2301–2308.
 (17) (a) Day, P. *J. Chem. Soc., Dalton Trans.* **1997**, 701–705. (b) Mathonière, C.; Nuttall, C. J.; Carling, S. G.; Day, P. *Inorg. Chem.* **1996**, *35*, 1201–1206. (c) Carling, S. G.; Mathonière, C.; Day, P.; Abdul Malik, K. M.; Coles, S. J.; Hursthouse, M. B. *J. Chem. Soc., Dalton Trans.* **1996**, 1839–1843.
 (18) (a) Coronado, E.; Galan-Mascaros, J. R.; Gomez-Garcia, C. J. *Synth. Met.* **1999**, *102*, 1459–1460. (b) Clemente-Léon, M.; Coronado, E.; Galan-Mascaros, J. R.; Gomez-Garcia, C. J. *J. Chem. Soc., Chem. Commun.* **1997**, 1727–1728.
 (19) Atovmyan, L. O.; Shilov, G. V.; Lyubovskaya, R. N.; Zhilyaeva, E. I.; Ovanesyan, N. S.; Pirumova, S. I.; Gusakovskaya, I. G.; Morozov, Y. G. *JETP Lett.* **1993**, *58*, 766–769.
 (20) Bénard, S.; Pei, Y.; Coradin, T.; Rivière, E.; Nakatani, K.; Clément, R. *Adv. Mater.* **1997**, *9*, 981–984.

- (21) (a) Atovmyan, L. O.; Shilov, G. V.; Lyubovskaya, R. N.; Zhilyaeva, E. I.; Ovanesyan, N. S.; Bogdanova, O. A.; Perumova, S. I. *Russian J. Coord. Chem.* **1997**, *23*, 640–642. (b) Shilov, G. V.; Atovmyan, L. O.; Ovanesyan, N. S.; Pyalling, A. A.; Botlyan, L. *Russ. J. Coord. Chem.* **1998**, *24*, 288–294.
 (22) Decurtins, S.; Schmalte, H. W.; Schneuwly, P.; Ensling, J.; Gütlich, P. *J. Am. Chem. Soc.* **1994**, *116*, 9521–9528.
 (23) Bällar, J. C.; Jones, E. M. *Inorg. Synth.* **1939**, *1*, 37–38.
 (24) (a) Broomhead, J. A.; Young, C. G. *Inorg. Synth.* **1982**, *21*, 127–128. (b) Burstall, F. H. *J. Chem. Soc.* **1936**, 173–175.
 (25) Constable, E. C.; Holmes, J. M. *J. Organomet. Chem.* **1986**, *301*, 203–208.
 (26) (a) Dwyer, F. P.; Sargeson, A. M. *J. Phys. Chem.* **1956**, *60*, 1331–1332. (b) Kauffman, G. B.; Takahashi, L. T.; Sugisaka, N. *Inorg. Synth.* **1966**, *8*, 207–208.
 (27) Dwyer, F. P.; Gyarfás, E. C. *J. Proc. R. Soc. N. S. W.* **1949**, *83*, 174–176.
 (28) Brissard, M.; Gruselle, M.; Malézieux, B.; Thouvenot, R.; Guyard-Duhayon, C.; Convert, O. *Chem. Eur. J.* **2001**, 1745–1751.

Table 1. Crystal Data for 1 and 2

formula	C ₃₆ H ₂₄ ClCrMnN ₆ O ₁₆ Ru	C ₃₇ H ₂₄ CrMnN ₅ O ₁₂ Ru
fw	1041.1	938.6
a (Å)	15.490(1)	15.368(5)
V (Å ³)	3716.7(5)	3627(2)
Z	4	4
cryst syst	cubic	cubic
space group	P2 ₁ 3	P2 ₁ 3
linear abs coef μ (cm ⁻¹)	11.51	10.9
ρ (g cm ⁻³)	1.86	1.72
diffractometer	IPDS Stoe	CAD4 Enraf–Nonius
radiation	Mo Kα (λ = 0.71069 Å)	Mo Kα (λ = 0.71069 Å)
scan type	ω/2θ	ω/2θ
scan range (°)	0.8 + 0.345t gθ	0.8 + 0.345t gθ
θ limits (°)	1.86–24.15	1–25
temp	160 K	295 K
octants collected	–17, 17; –17, 17; –17, 17	0, 18; 0, 18; 0, 18
nb of data collected	24039	3583
nb of unique data collected	1116	1193
nb of unique data used	600 (F _o) ² > 3σ(F _o) ²	509 (F _o) ² > 2σ(F _o) ²
R ^a	0.0575	0.0409
R _w ^b	0.0651	0.0419
GOF	1.10	1.23
extinction parameter	none	none
nb of variables	88	83

$$^a R = [\sum(|F_o| - |F_c|)/\sum F_o]. \quad ^b R_w = [\sum w(|F_o| - |F_c|)^2/\sum w F_o^2]^{1/2}.$$

is a HeNe laser emitting at 632.8 nm. Due to the absorption of the material, the sample consists of KBr polished pellets containing 0.1 w% of finely grounded material.

Synthesis of Optically Active {[Ru(bpy)₃][ClO₄][MnCr(ox)₃]}_n 1. The corresponding 1-Δ and 1-Λ enantiomers were obtained by crystallization in a tetramethoxysilane gel using optically active Δ or Λ [Ru(bpy)₃]²⁺ derivatives: Δ [Ru(bpy)₃]₂ [α_D]²⁰ = –768 (C 0.08, H₂O), ee = 0.94; Λ [Ru(bpy)₃]₂ [α_D]²⁰ = +824 (C 0.08, H₂O), ee = 1.00. The obtention of 1-Δ is described in detail as an example.

{[ΔRu(bpy)₃][ClO₄][ΔMnΔCr(ox)₃]}_n 1-Δ. A tetramethoxysilane gel is formed by mixing Si(OMe)₄ (5 cm³) and MeOH (5 cm³) and posterior addition of an aqueous solution (5 cm³) containing 70 mg (0.16 mmol) of [NH₄][Cr(ox)₃]₂·3H₂O. The solution was homogenized and distributed into five test tubes. After a few days the gel is formed, and 10 cm³ of a mixture of water–acetone (1:1) containing 150 mg of [ΔRu(bpy)₃]₂·6H₂O, 35 mg of MnCl₂·4H₂O, and two drops of HClO₄ was added. After two weeks, the red crystals formed inside the gel were hand picked (2–5 mg from each tube). IR (KBr): 1647, s; 1619, vs; 1377, m; 1095, s; 814, m; 770, m; 541, m; 476, m; 420, m. Anal. Calcd for C₃₆H₂₄N₆O₁₆ClCrMnRu: C, 41.57; H, 2.33; N, 8.08. Found: C, 38.47; H, 2.40; N, 7.20. Suitable crystals for X-ray diffraction studies were obtained for {[ΔRu(bpy)₃]²⁺, ClO₄⁻, [ΔMn^{III}ΔCr^{III}(ox)₃]⁻}_n 1-Δ.

Synthesis of Racemic and Optically Active {[Ru(bpy)₂ppy]-[M Cr(ox)₃]}_n (M = Mn, Ni) 2-Δ, 2-Λ, and 3-Δ, 3-Λ. The procedure of obtention of racemic {[Ru(bpy)₂ppy][M Cr(ox)₃]}_n (M = Mn, Ni) 2, 3-rac in high yield and purity illustrates the methodology followed to prepare their optically active forms.

{[Ru(bpy)₂ppy][MnCr(ox)₃]}_n 2-rac. An aqueous solution (2 cm³) containing 25 mg of [NH₄]₃[Cr(ox)₃]₂·3H₂O (0.06 mmol) and 12 mg of MnCl₂·4H₂O (0.06 mmol) was added with stirring to a solution of [Ru(bpy)₂ppy][PF₆] (43 mg, 0.06 mmol) in 10 cm³ of acetone. A precipitate started to appear after a few minutes, and, after 1 h, it was filtered off, washed with water and acetone, and air-dried to yield 46 mg (81%) of a violet solid characterized as {[Ru(bpy)₂ppy][MnCr(ox)₃]}_n 2. IR (KBr): 1643, s; 1623, vs; 1436, m; 1296, m; 811, m; 767, m; 543, m; 477, m; 418, m. Anal. Calc. for C₃₇H₂₄N₅O₁₂-CrMnRu: C, 47.35; H, 2.58; N, 7.46; Cr, 5.54; Mn, 5.85; Ru, 10.77. Found: C, 45.44; H, 2.53; N, 6.74; Cr, 5.41; Mn, 5.79; Ru, 8.67.

{[Ru(bpy)₂ppy][NiCr(ox)₃]}_n 3-rac. This compound was prepared as described above with NiCl₂·6H₂O. A violet solid was obtained in an 85% yield and characterized as {[Ru(bpy)₂ppy][NiCr(ox)₃]}_n. IR (KBr): 1623, vs; 815, m; 764, m; 545, m; 476, m. Anal. Calc. for C₃₇H₂₄N₅O₁₂-CrNiRu: C, 47.16; H, 2.57; N, 7.43; Cr, 5.52; Ni, 6.23; Ru, 10.72. Found: C, 43.15; H, 2.62; N, 6.82; Cr, 4.58; Ni, 8.00; Ru, 8.15.

The synthesis described above for the obtention of the racemic compounds was followed for the preparation of the corresponding optically active derivatives 2-Δ, 2-Λ and 3-Δ, 3-Λ, using (1.) resolved K₃Cr(ox)₃·3H₂O; Δ K₃Cr(ox)₃·3H₂O [α_D]²⁰ = –1800 (C 0.04, H₂O), lit: (–1940) or Λ K₃Cr(ox)₃·3H₂O [α_D]²⁰ = +1932 (C 0.04, H₂O), lit: (+1928) and a double proportion of racemic [Ru(bpy)₂ppy]PF₆. In this case, to avoid racemization of K₃Cr(ox)₃, only the insoluble product formed in the first 5 mn was collected (30% yield); (2.) resolved [Ru(bpy)₂ppy]PF₆; Δ [Ru(bpy)₂ppy]PF₆ ee = 0.44 or Λ [Ru(bpy)₂ppy]PF₆ ee = 0.50 (ee were calculated according to ref 24) and a double proportion of racemic K₃Cr(ox)₃·3H₂O. [Ru(bpy)₂ppy]⁺ does not racemize in solution; thus, the final products can be obtained in good yields but their enantiomeric excess cannot be high because of the partial resolution of the starting monocation.

Crystal Growth. Single crystals of {[Ru(bpy)₂ppy][MnCr(ox)₃]}_n 2-Λ were obtained from racemic reagents by crystallization in a tetramethoxysilane gel containing (NH₄)Cr(ox)₃·3H₂O (0.03M). When the gel is formed, the stoichiometric quantities of a MeOH–acetone (1:1) solution containing [Ru(bpy)₂ppy]PF₆ and MnCl₂·4H₂O were added. After one week, the dark octahedral shaped crystals of {[ΔRu(bpy)₂ppy][ΔMnΔCr(ox)₃]}_n 2-Λ are formed. When the same conditions are used to crystallize {[Ru(bpy)₂ppy][NiCr(ox)₃]}_n 3, only microcrystalline samples have been obtained.

X-ray Crystallographic Analysis for {[ΔRu(bpy)₃]²⁺, ClO₄⁻, [ΔMn^{III}ΔCr^{III}(ox)₃]⁻}_n 1-Δ and {[Ru(bpy)₂ppy]⁺, [ΔMn^{III}ΔCr^{III}(ox)₃]⁻}_n 2-Λ. Data were collected on a Stoe Imaging Plate Diffraction System for 1-Δ and on an Enraf–Nonius CAD4 diffractometer for 2-Λ. In both cases no significant decay was observed. Crystal parameters and collection details are summarized in Table 1. The data were corrected for Lorentz and polarization effects. Computations were performed using the PC version of CRYSTALS.²⁹ Scattering factors and corrections for anomalous absorption were taken from ref 30. The structures were solved by direct methods (SHELXS).³¹ Last refinements were carried out by full-matrix least-squares using isotropic displacement parameters (except for Ru, Cr, and Mn atoms for 2-Λ). Hydrogen atoms were introduced in a calculated position and allocated one overall isotropic displacement parameter. For compound 2-Λ, the space group (P2₁3) would require that the three ligands around Ru are identical,

(29) Watkin, J.; Prout, C. K.; Carruthers, J. R.; Betteridge, P. W. *CRYSTALS*, Issue 10 D; Chemical Crystallography Laboratory: University of Oxford, U.K., 1996.

(30) *International Tables for X-ray Crystallography*; Kynoch Press: Birmingham, England, 1974; Vol. IV.

(31) Sheldrick, G. M. *Shelxs86*, Program for Crystal Structure Solution; University of Göttingen: Germany, 1986.

that is not true. The observed symmetry is only a pseudo symmetry due to the fact that the phenylpyridine and the two bipyridine ligands are randomly distributed around each ruthenium atom. The presence of the phenylpyridine ligand is not directly pointed out, but it is undoubtedly confirmed by the absence of free anions.

Crystallographic data (excluding structure factors) for the structures reported in this paper have been deposited with the Cambridge Crystallographic Data center as supplementary publication nos. CCDC 155070 and CCDC 155071 for 1- Δ and 2- Λ , respectively. Copies of the data can be obtained free of charge on application to CCDC, 12 Union Road, Cambridge CB21EZ, UK (Fax: (+44)1223-336-033; E-mail: deposit@ccdc.cam.ac.uk).

Results and Discussion

Up to date bidimensional networks of general formula $\{[A]-[M^II M^III(ox)_3]_n\}$ have been obtained with achiral cations. The interactions between such cations and the Δ or Λ configurations of the anionic subunits “[M(ox)₃]³⁻” are essentially the same, and both configurations are present in the crystal structure. The arrangement of alternating Δ and Λ configurations gives rise to a layered structure with the cations located between the honeycomb layers $\{[M^II M^III(ox)_3]_n\}$. When a chiral cation is present, specific interactions can be established with the Δ or Λ configuration of the [M(ox)₃]³⁻ ions, as in a classical enantiomeric resolution process, inducing the homochiral assembly of the subunits necessary in the construction of a three-dimensional 3-connected 10-gon (3,10) network. The chiral or achiral character of the cations can be a determining factor in the formation of a 2D or 3D system.

The synthesis of a 3D network of general formula $\{[A]-[M^II M^III(ox)_3]_n\}$ requires a chiral monocation of appropriate size and shape. When such chiral cations can be resolved into configurationally stable enantiomers, the enantioselective synthesis of optically active materials is envisageable.

Two different synthetic strategies have been followed in the preparation of this new kind of compound. We first tried the synthesis with a chiral dication, like [Ru(bpy)₃]²⁺, in association with a monoanion to reduce the positive charge in one unity to compensate for the charge of the anionic network $\{[M^II M^III(ox)_3]_n\}$. We have also explored the ability of a monocation like [Ru(bpy)₂ppy]⁺, with similar size and the same helical chirality as [Ru(bpy)₃]²⁺, to act as template in the formation of these new three-dimensional bimetallic oxalate-bridged networks. In both cases, the use of resolved chiral reagents leads to the enantioselective synthesis of optically active products.

To build optically active 2D and 3D networks in a rational way, two configurational elements must be controlled: (i) the absolute Δ or Λ configuration of each chiral hexacoordinated metal center and (ii) the relative configuration between two adjacent metal centers. The first condition determines the optical activity. Resolving the starting building blocks can fulfill it. The second condition determines the dimensionality of the network. A heterochiral arrangement, i.e. ($\Delta M_1, \Lambda M_2$) or ($\Lambda M_1, \Delta M_2$), leads to a 2D network; the anionic sublattice displays a honeycomb structure, while the cationic moiety, which usually is a tetra-alkylammonium (NR₄⁺) ion, a phosphonium (PR₄⁺) ion, or a thio derivative (BEDT-TFF)⁺, is located between the anionic layers.^{15–21}

On the other hand, a homochiral arrangement, i.e., ($\Delta M_1, \Delta M_2$) or ($\Lambda M_1, \Lambda M_2$), leads to a 3D network built from a [3-connected 10-gon] anionic network, while the associated cationic counterpart, possessing the same *D*₃ symmetry as that of the connected metal centers, fits in the vacancies.²²

We found that the treatment of resolved $[\Delta Cr^III(ox)_3]^{3-}$ or $[\Lambda Cr^III(ox)_3]^{3-}$ with Mn²⁺ in the presence of ammonium

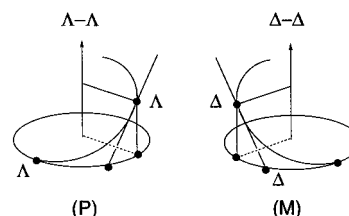
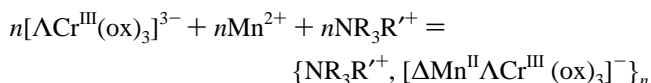
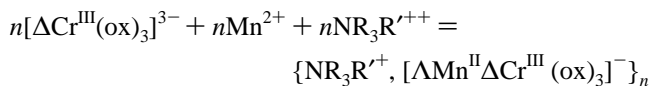


Figure 2. Relationship between the configuration from the molecular to the supramolecular level for helices built from bricks of *D*₃ symmetry.

derivatives NR₃R⁺ afforded optically active 2D networks:³²



Circular dichroism curves support the enantiomeric character of the obtained $\{NR_3R^{++}, [\Delta Mn^II \Delta Cr^III(ox)_3]^{-}\}_n$ and $\{NBu_4^+, [\Delta Mn^II \Lambda Cr^III(ox)_3]^{-}\}_n$ compounds.

These initial results clearly illustrate the idea that in the formation of highly ordered networks, control over the chirality (absolute configuration) of at least one of the chiral building blocks allows for control of the overall chirality of the network. In the above example, the only required condition to build up optically active 2D networks is encoded in the absolute configuration of the resolved starting anionic brick, i.e. [Cr(ox)₃]³⁻.

In the case of 3D networks, the homochiral arrangement of the bimetallic framework displays a helical structure. The right or left twist of the helices depends on the absolute configuration of the connected metal centers, namely M for Δ and P for Λ (Figure 2).

As reported previously, the cationic entity acts as a structural (dimensionality, 2D or 3D) and chiral (absolute configuration, optical activity) template. Decurtins showed that in the polymeric compounds $\{Fe(bpy)_3\}^{2+}$, $\{Li^I Cr^III(ox)_3\}^{2-}$ (bpy = 2,2'-bipyridine), the chiral cationic counterpart presents the same configuration as the oxalate bridged metals.²²

Therefore, the orientation toward 3D networks depends on the symmetry of the counteranion, when its charge and size are appropriate. Thus, using the configurationally stable resolved dication Δ or Λ [Ru(bpy)₃]²⁺ in the presence of the other reagents (LiCl, rac-K₃Cr(ox)₃), we obtained in crystalline forms the two enantiomeric systems $\{\Delta Ru(bpy)_3\}^{2+}$, $[\Delta Li^I \Delta Cr^III(ox)_3]^{2-}$ or $\{\Lambda Ru(bpy)_3\}^{2+}$, $[\Lambda Li^I \Lambda Cr^III(ox)_3]^{2-}$. The absolute configuration of each metal center and the M and P helices were determined by NCD studies and X-ray diffraction.³² Similarly, when starting from the resolved tris(oxalato)chromate and racemic cationic template, we obtained the same optically active polymers, i.e. the configuration of the homochiral 3D network assembly can be controlled either by the configuration of the hexacoordinated anionic building block ([Cr(ox)₃]³⁻) or by that of the cationic template ([Ru(bpy)₃]²⁺).

The structural objective of the work, i.e. obtaining enantiomerically pure M or P helices, is thus achieved in a 3D system.

(32) (a) Andrés, R.; Gruselle, M.; Malézieux, B.; Verdager, M.; Vaissermann, J. *Inorg. Chem.* **1999**, *38*, 4637–4646. (b) Malézieux, B.; Román, A.; Brissard, M.; Gruselle, M.; Train, C.; Herson, P.; Troitskaya, L. L.; Sokolov, V. I.; Ovseenko, S. T.; Demeschik, T. V.; Ovanessian, N. S.; Mamed'yarova, I. A. *J. Organomet. Chem.*, submitted for publication.

Table 2. Selected Bond Lengths (Å) and Bond Angles (Deg) for **1**

Ru(II) environment		Cr(III) environment	
Ru(1)–N(1)	2.05(1)	Cr(1)–O(3)	2.24(1)
Ru(1)–N(2)	2.03(1)	Cr(1)–O(4)	2.27(1)
N(1)–Ru(1)–N(1) ^a	94.4(5)	O(3)–Cr(1)–O(3) ^e	91.3(5)
N(1)–Ru(1)–N(2)	79.1(4)	O(3)–Cr(1)–O(4)	74.6(4)
N(1)–Ru(1)–N(2) ^b	171.6(5)	O(3)–Cr(1)–O(4) ^d	165.6(5)
N(1)–Ru(1)–N(2) ^c	91.5(5)	O(3)–Cr(1)–O(4) ^e	91.9(5)
N(2)–Ru(1)–N(2) ^b	95.6(5)	O(4)–Cr(1)–O(4) ^d	102.4(4)
Mn(II) environment		oxalate ligand	
Mn(1)–O(1)	1.97(1)	O(1)–C(1)	1.31(2)
Mn(1)–O(2)	1.98(1)	O(2)–C(2)	1.30(2)
O(1)–Mn(1)–O(1) ^e	90.1(5)	O(3)–C(1)	1.20(2)
O(1)–Mn(1)–O(2)	83.2(5)	O(4)–C(2)	1.25(2)
O(1)–Mn(1)–O(2) ^f	93.1(6)	C(1)–C(2)	1.54(2)
O(1)–Mn(1)–O(2) ^e	172.6(5)		
O(2)–Mn(1)–O(2) ^f	94.0(5)		

^a y, z, x . ^b z, x, y . ^c $1 - y, 1/2 + z, 1/2 - x$. ^d $1/2 - z, 1 - x, -1/2 + y$. ^e $-1/2 + y, 1/2 - z, -x$. ^f $-z, 1/2 + x, 1/2 - y$.

Table 3. Selected Bond Lengths (Å) and Bond Angles (Deg) for **2**

Ru(II) environment		Cr(III) environment	
Ru(1)–N(1)	2.04(1)	Cr(1)–O(1)	2.09(1)
Ru(1)–N(2)	2.02(1)	Cr(1)–O(3)	2.10(1)
N(1)–Ru(1)–N(1) ^a	95.4(5)	O(1)–Cr(1)–O(1) ^e	91.3(5)
N(1)–Ru(1)–N(2)	79.2(4)	O(1)–Cr(1)–O(3)	77.8(4)
N(1)–Ru(1)–N(2) ^b	173.3(4)	O(1)–Cr(1)–O(3) ^d	92.3(4)
N(1)–Ru(1)–N(2) ^a	89.1(5)	O(1)–Cr(1)–O(3) ^e	168.6(4)
N(2)–Ru(1)–N(2) ^b	96.6(5)	O(3)–Cr(1)–O(3) ^d	99.1(4)
Mn(II) environment		oxalate ligand	
Mn(1)–O(2)	2.10(1)	O(1)–C(11)	1.22(2)
Mn(1)–O(4)	2.08(1)	O(2)–C(11)	1.25(2)
O(2)–Mn(1)–O(2) ^e	90.9(4)	O(3)–C(12)	1.25(2)
O(2)–Mn(1)–O(4)	78.1(4)	O(4)–C(12)	1.26(2)
O(2)–Mn(1)–O(4) ^f	91.6(4)	C(11)–C(12)	1.53(2)
O(2)–Mn(1)–O(4) ^e	168.8(4)		
O(4)–Mn(1)–O(4) ^f	99.6(4)		

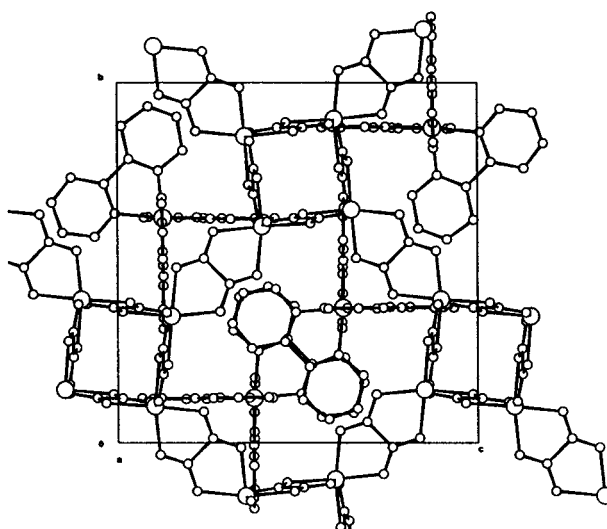
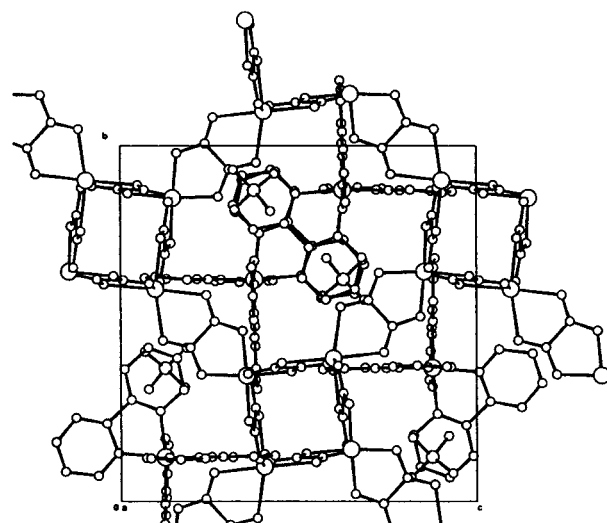
^a y, z, x . ^b z, x, y . ^c $1/2 + z, 3/2 - x, 1 - y$. ^d $3/2 - y, 1 - z, -1/2 + x$. ^e $1/2 + y, 1/2 - z, 1 - x$. ^f $1 - z, -1/2 + x, 1/2 - y$.

On the contrary, the magnetic goal remains to be reached, since the diamagnetic lithium ion associated with a chromium(III) ion in such 3D networks leads to paramagnetic materials.

To get a long-range magnetically ordered solid, one must create a bimetallic system in which tandems of transition paramagnetic ions such as (Mn^{II}, Cr^{III}) or (Ni^{II}, Cr^{III}) present an exchange interaction through the oxalate bridge in a 3D network. In such compounds, the anionic subunit [M^{II}M^{III}(ox)₃][−] bears one negative charge. To be able to follow the strategy proposed above to get a 3D structure, the *D*₃ symmetry template of appropriate size must bear one positive charge. Such single charged species can be obtained by two chemical ways. (i.) Associate a configurationally stable dication such as [Ru(bpy)₃]²⁺ to a monoanion to obtain a global monocationic charge. Decurtins was the first to propose the use of a tandem [Cr^{III}(bpy)₃]³⁺/ClO₄[−] as a template to obtain 3D paramagnetic [Cr–Na] networks,³³ whereas Julve used the same approach to get an homobimetallic Co^{II} 3D network which is a canted antiferromagnet.⁷ (ii.) Using monocationic species such as [Ru(bpy)₂ppy]⁺ (ppy = phenylpyridine), reported previously.²⁴ This monocation is close in structure and size to [Ru(bpy)₃]²⁺ and possesses a quasi *D*₃ symmetry.³⁴

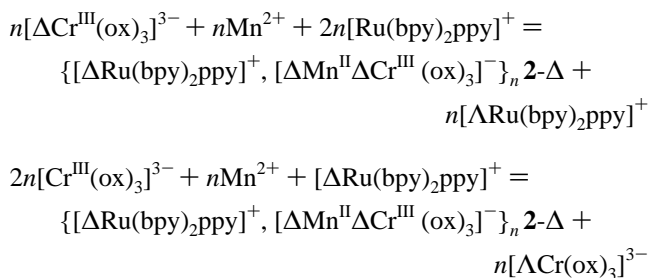
(33) Decurtins, S.; Schmalte, H. W.; Pellaux, R.; Schneuwly, P.; Hauser, A. *Inorg. Chem.* **1996**, *35*, 1451–1460.

(34) The symmetry of the monocation [Ru(bpy)₂ppy]⁺ is formally *C*₁. Nevertheless, according to the external shell geometry which is very close to that of [Ru(bpy)₃]²⁺, one can assume for the monocation a quasi *D*₃ symmetry.

**Figure 3.** Perspective views of one helix of the anionic sublattice for compounds (a) **1** and (b) **2**.

Following these two strategies, we obtained the following optically active networks: {[Ru(bpy)₃]²⁺, ClO₄[−], [Mn^{II}Cr^{III}(ox)₃][−]]_n **1** and {[Ru(bpy)₂ppy]⁺, [M^{II}Cr^{III}(ox)₃][−]]_n with M^{II} = Mn^{II} **2**, Ni^{II} **3**.

As previously described for the [Li–Cr]-3D systems,³² the optically active 3D networks **1-Δ**, **1-Λ**; **2-Δ**, **2-Λ**; and **3-Δ**, **3-Λ** can be prepared using resolved anionic building blocks or a resolved cationic template, as shown as an example for **2-Δ** in the following equations:



X-ray Structural Studies. Suitable crystals for X-ray diffraction studies were obtained for compound **1-Δ** and **2-Λ** using a gel technique. The unit cells are enantiomorphic: (*P*2₁3) for **1-Δ** and **2-Λ**.²⁵ Crystal data and structure determination parameters are shown in Table 1. Selected angles and bond

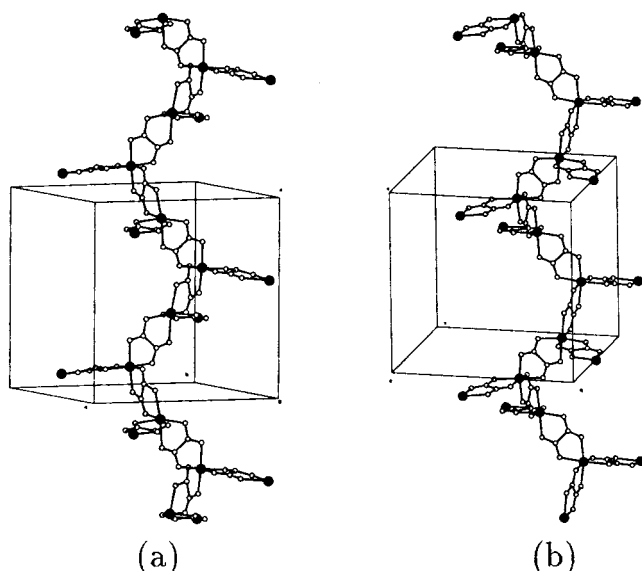


Figure 4. CAMERON view along the *a* axis of the unit cell for compounds (a) **1** and (b) **2**.

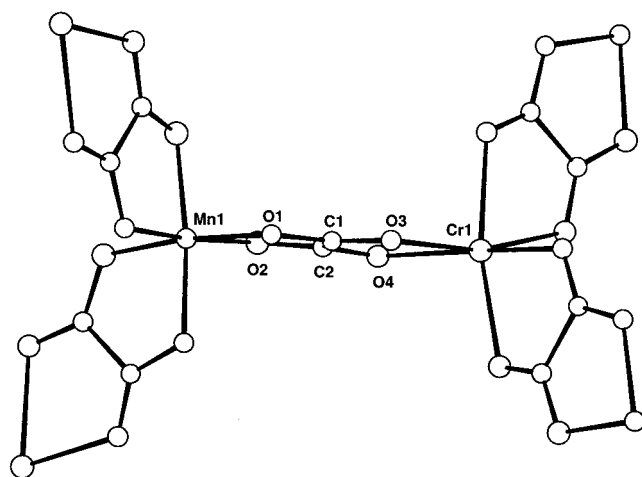


Figure 5. CAMERON drawing with the labeling scheme of the Mn and Cr coordination of the compounds **1** and **2**.

lengths are listed in Tables 2 and 3. In these structures, all metallic centers show the same configuration Δ for **1- Δ** and Λ for **2- Λ** , leading to anionic helices of configuration M and P, respectively. The topology of these compounds shows the expected chiral three-dimensional 3-connected 10-gon (10,3) network configuration with the formal $[M(\text{ox})_3/2]$ units representing three connecting nodes. The oxalate ligands bridge the adjacent transition metal ions M_1^{II} , M_2^{III} in all three dimensions, leading to a bimetallic 3D ordered network. Respective positions of chromium and manganese were attributed by taking into consideration the optimal value of the R factor. The cations, $[\Delta\text{Ru}(\text{bpy})_3]^+$ associated to the ClO_4^- anion for **1- Δ** and $[\Lambda\text{Ru}(\text{bpy})_2\text{ppy}]^+$ for **2- Λ** , respectively, fit the vacancies of the anionic networks. Perspective views of one helix of the anionic sublattice for **1- Δ** and **2- Λ** are shown in Figure 3. The two structures are very similar. The most significant difference lies in the size of the unit cell: 14.490 and 15.368 \AA^3 for **1- Δ** and **2- Λ** , respectively. Additionally, one can observe that the oxalate ligand in **2- Λ** is more symmetric and more symmetrically bonded to the transition metal ions (2.08, 2.10, 2.09, and 2.10 \AA) than in **1- Δ** (1.97, 1.98, 2.24, and 2.27 \AA). This point will be further discussed together with the magnetic properties.

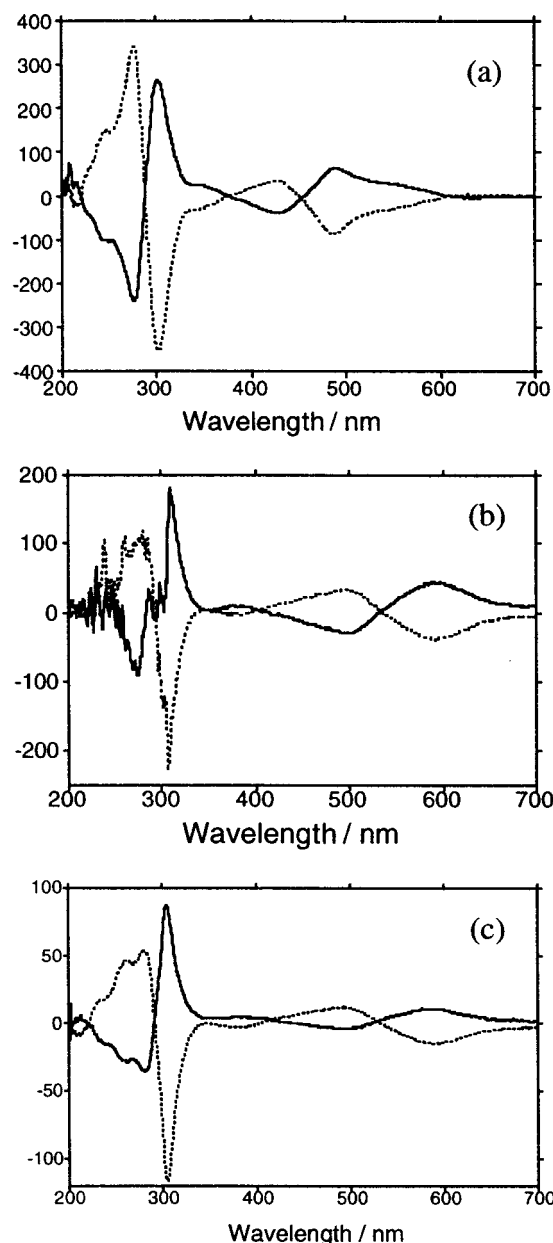


Figure 6. NCD curves of the two enantiomeric forms of (a) **1**, (b) **2**, and (c) **3**. The Λ enantiomer appears in a straight line while the Δ enantiomer appears in a dashed line

CAMERON views³⁵ of **1- Δ** and **2- Λ** along the *c* axis of the unit cell are shown in Figure 4a,b. A chromium–manganese unit $[\text{Cr}-\text{Mn}]$ connected by an oxalate ligand is shown in Figure 5.

Cotton Effects. The natural circular dichroism (NCD) curves shown in Figure 6 establish the enantiomeric character of the obtained **1- Δ** , **1- Λ** ; **2- Δ** , **2- Λ** ; and **3- Δ** , **3- Λ** networks. Absolute configurations for Ru and Cr centers were determined by comparison of their NCD spectra with those of Δ and Λ enantiomers of $[\text{Cr}^{\text{III}}(\text{ox})_3]^{3-}$,²⁶ $[\text{Ru}(\text{bpy})_2\text{ppy}]^+$,²⁷ and $[\text{Ru}(\text{bpy})_3]^{2+}$,²⁸ following the principle that two related optically active molecules have the same absolute configuration if they give a Cotton effect of the same sign in the absorption wavelength region of an electronic transition common to both molecules.³⁶ Due to the extremely low solubility of the obtained

(35) Watkin, D. J.; Prout, C. K.; Pearce, L. J. *CAMERON*; Chemical Crystallography Laboratory: University of Oxford, U.K., 1996.

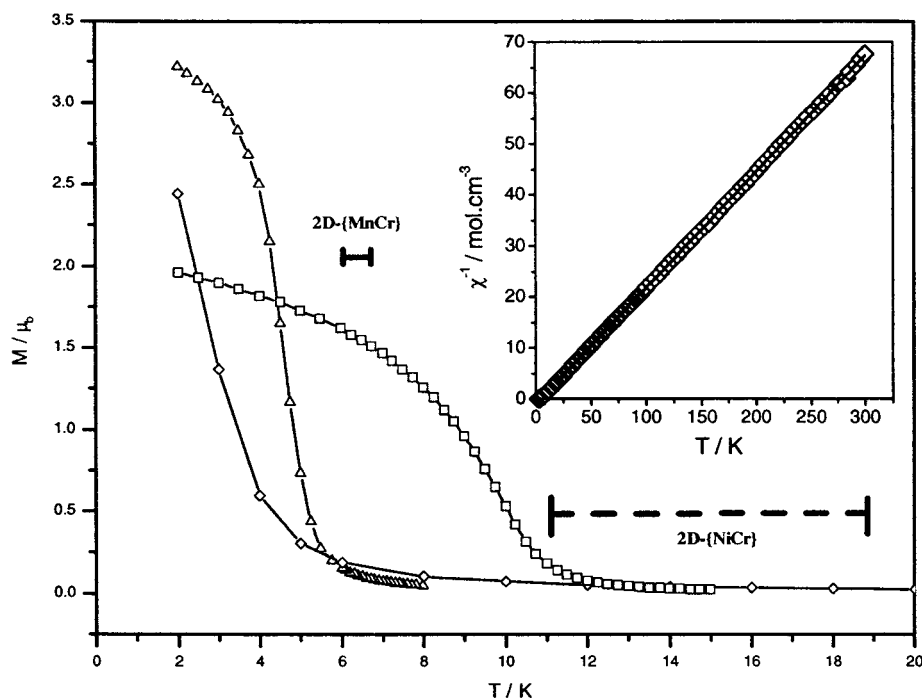


Figure 7. Field-cooled (FC) curves for compound **1** (\diamond), **2** (Δ), and **3** (\square). The T_c measured for the [Mn–Cr]^{11b} and [Ni–Cr]^{17a} 2D compounds fall into the black segments. The insert shows the experimental $(\chi_M)^{-1}$ versus T curve and its fit for compound **2**.

polymers, solid state circular dichroism was imposed. All bands are essentially due to intra-ligand or MLCT transitions of [Ru-(bpy)₃]²⁺³⁷ for **1-Δ**, **1-Λ** or [Ru(bpy)₂ppy]⁺²⁸ for **2-Δ**, **2-Λ** and **3-Δ**, **3-Λ**. A positive Cotton effect at $\lambda = 300$ nm is representative of a Δ configuration for the Ru(II) compound. In the case of **1-Δ**, **1-Λ**, typical signals of a Cr^{III} complex^{36b,38} (shoulder at $\lambda = 570$ nm) can also be observed in the high wavelength region.

Magnetic Properties. The $\chi_M T$ values at 300 K of compounds **2** and **3** are close to the spin-only value for two independent metal ions (6.25 for **1** and **2** and 2.875 for **3**). The difference observed for **1** might be attributed to diamagnetic gel residues. The three $\chi_M T$ curves show a monotonic increase with decreasing T . As shown in the insert of Figure 7 for compound **2**, the χ_M^{-1} versus T curves are linear in the 30–250 K temperature range. They can be fitted by a Curie–Weiss law $\chi_M^{-1} = (T - \Theta)/C$. The Weiss constants are positive and equal to +4.4, 6.0, and 17.7 K for **1**, **2**, and **3**, respectively. The $\chi_M T$ curves are monotonic. Moreover, at low temperature they diverge, demonstrating the onset of a long-range magnetic order. The Curie temperature T_c is given by the intersection of the linear fit of the steepest part of the field-cooled curve obtained in 0.01 T with the T axis. The Curie temperatures for **1**, **2**, and **3** are respectively 4.2, 5.8, and 11.0 K (Figure 7). The hysteresis loops at 2 K show that these compounds are soft magnets with hardly measurable coercive forces.

Both the shape of the $\chi_M T$ versus T curves and the sign of Weiss constants indicate the existence of a short-range ferromagnetic interaction between the paramagnetic ions in the three compounds. Ferromagnetism was also observed in the 2D

compounds,^{15b,21a} and the T_c values for the 2D and 3D compounds are close (Figure 7). Moreover, within experimental error, neither T_c nor Θ depend on the absolute configuration of the compounds.

These observations are consistent with the orbital approach widely used to explain the exchange interaction in molecule-based magnets.^{1,4,39} The J is actually determined by the overlap and orthogonality of magnetic orbitals of two oxalate-bridged metallic ions in a pseudo-octahedral environment,³⁹ and the number of neighbors are independent of the dimensionality of the compound. Following this scheme, the variation of T_c can be tentatively related to subtle changes in geometry within the basic motif of the network. Hence, the crystallographic study shows that the oxalate bridge in **1** is rather unsymmetrical, leading to a weakening of delocalization on the carboxylate groups in **1** compared to **2**. This could explain the decrease of T_c . Further magnetostructural studies, including theoretical calculations, will be needed to precisely define such correlation.

Moreover, there exists a sharp contrast between the coercive force of **3** compared to those of Ni–Cr 2D networks assembled with trialkyl(ferrocenylmethyl)ammonium.^{32b} Going from 2D to 3D networks, one experiences a sharp decrease of magnetocrystalline anisotropy.⁴⁰ In the 3D compounds, the cubic anisotropy is easily overcome. This leads to low coercive forces compared to those of the 2D case.

The magnetic measurements establish that we have synthesized the first optically active ferromagnets. This result is illustrated by the magneto-optical behavior of compound **1** presented in Figure 8. Magnets are able to show noticeable magnetic circular dichroism (MCD) below their Curie temperature.

The hysteresis loop for compound **1** was measured at 2.17 K, e.g., below its T_c , in fields up to 0.1 T (Figure 8). The result

(36) (a) Richardson, F. S. *Chem. Rev.* **1979**, 79, 17–36. (b) McCaffery, A. J.; Mason, S. F.; Ballard, R. E. *J. Chem. Soc.* **1965**, 2883–2892. (c) Ziegler, M.; Von Zelewsky, A. *Coord. Chem. Rev.* **1998**, 177, 257–300.

(37) McCaffery, A. J.; Mason, S. F.; Norman, B. J. *J. Chem. Soc. A*: **1969**, 1428–1441.

(38) Gillard, R. D.; Shepherd, D. J.; Tarr, D. A. *J. Chem. Soc., Dalton Trans.* **1976**, 594–599.

(39) Ohba, M.; Tamaki, H.; Matsumoto, N.; Okawa, H. *Inorg. Chem.* **1993**, 32, 5385–5390. (b) Pei, Y.; Journaux, Y.; Kahn, O. *Inorg. Chem.* **1989**, 28, 100–103.

(40) Kittel, C. *Introduction à la Physique de l'Etat Solide* Dunod: Paris, 1972.

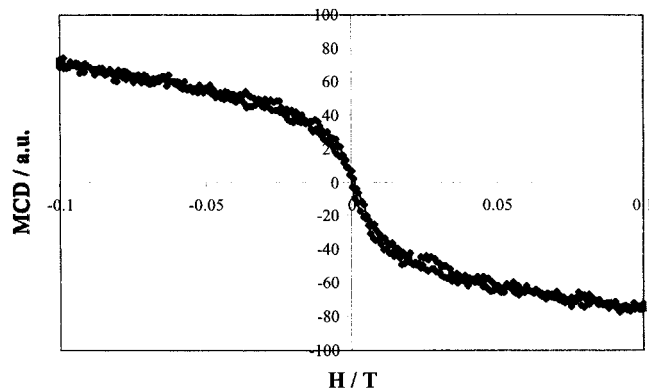


Figure 8. Magnetic circular dichroism (MCD) measured at 2.17 K on a KBr pellet containing 0.1% of compound **1**.

hardly depends on the enantiomer. Due to several scattering sources and to the dilution of the compound in the KBr matrix, the dichroic signal is rather weak, but the loop is nevertheless one of the first ever published for a molecule-based magnet.⁴¹

The MCD signal is linked to the existence of a nonzero magnetization component along the direction of the light beam propagation. Neither its intensity nor its sign depend on the optical activity of the compound. It adds (algebraically) to the NCD shown in Figure 6. This experiment, together with the observed NCD signal, shows the capability of these compounds to exhibit an important magnetochiral effect,⁴² a cross effect that arises from the coexistence of magnetic properties and structural chirality in the system. Moreover, the enantiospecificity of this synthetic strategy may be applied to obtain compounds that would possess both magnetic and structural helicity, the latter being strictly controlled. The link between these two chiral structures could thus be deeply studied.

(41) Ohkoshi, S.; Mizuno, M.; Hung, G.; Hashimoto, K. *J. Phys. Chem B* **2000**, *104*, 9365–9367.

(42) (a) Baranova, N. B.; Zeldovich, B. Ya. *Mol. Phys.* **1979**, *38*, 1085–1098. (b) Wagnière, G. H.; Meier, A. *Chem. Phys. Lett.* **1982**, *93*, 78–81. (c) Barron, L. D.; Vrbancich, J. *Mol. Phys.* **1984**, *51*, 715–730.

Concluding Remarks

We have reported the synthesis and the magnetic, optical, and magneto-optical properties of the first optically active 3D magnets, rationally designed from molecular precursors.

Through the control over structural chirality, the presented synthetic strategy may bring new insights into fundamental magnetic problems concerning the link between magnetic and structural chiralities. Moreover, we have shown that these compounds present an important natural circular dichroism and a measurable magnetic circular dichroism.

This work opens up a new field of research in polyfunctional molecular materials exhibiting both magnetic and optical properties. Through these findings, the compounds actually appear to be good candidates to present an important cross-effect between NCD and MCD, the so-called magnetochiral dichroism (MChD).⁴² If any chiral system presents MChD, the effect is very weak for diamagnetic⁴³ and paramagnetic⁴⁴ systems due to their low magnetization. The signal presented by an optically active magnet, displaying a large magnetization and important MCD and NCD, should be considerably larger.

Acknowledgment. Authors thank CNRS (France), Université “Pierre et Marie Curie” (France), INTAS (n°96903) for financial support, and the Spanish “Ministerio de Educacion y Cultura” for a postdoctoral fellowship. Dr Jean Claude Daran is gratefully thanked for recording X-ray data of compound **2**. The authors also thank I. Rosenman (GPS, Paris) for easy access to his squid susceptometer. This article is a part of the Ph.D. work of Muriel Brissard.

IC010363F

(43) Kleindienst, P.; Wagnière, G. H. *Chem. Phys. Lett.* **1998**, *288*, 89–97.

(44) Rikken, G. L. J. A.; Raupach, E. *Nature (London)* **1997**, *390*, 493–494. (b) Rikken, G. L. J. A.; Raupach, E. *Phys. Rev. E* **1998**, *58*, 5081–5084.